Geomorphodiversity and anthropization indices for Italian urban areas

Martina Burnelli[a,b], Laura Melelli[a], Massimiliano Alvioli[b,*]

[a] *Department of Physics and Geology, University of Perugia, Perugia, Italy*
[b] *Consiglio Nazionale delle Ricerche, Istituto di Ricerca per la Protezione Idrogeologica, via Madonna Alta 126, I-06128 Perugia, Italy*

Abstract

Urban geomorphology analyzes modifications of morphology and topography induced by human activity in cities, urban and peri–urban areas. Urban expansion modifies ecosystems, but global actions for sustainability focus on the biosphere, overlooking the role of abiotic components, embedded in and supported by the geosphere and its ecosystem services.

We propose the joint study of indicators of land surface variability and of anthropic modifications. We consider geomorphodiversity, as a discrete measure of richness and variability of abiotic components, and a new index describing the degree of human impact inferred from land cover classes. We suggest that a joint study of the two indicators helps quantifying and understanding the effect of specific land cover changes on areas with different values of geomorphodiversity and the relationships between abiotic parameters and the human presence in urban areas.

Public datasets permits study geomorphology simultaneously at the national scale, and the local scale, within individual urban areas. We show that (1) urban development in Italy was fostered in lowlands, alluvial plains or hills, and urban areas with large values of geomorphodiversity host larger

[*] Corresponding Author. E–mail address: massimiliano.alvioli@irpi.cnr.it

numbers of natural areas; (2) different definitions of urban boundaries are essential to investigate different aspects of human impact on the landscape; (3) synthetic scenarios of land use change, corresponding to different values of anthropization, are useful to study the effect on geomorphodiversity.

Quantitative geomorphodiversity and anthropization index contain complementary information, and their joint study is an additional tool to plan city development and conservation of natural areas in a broad sense.

1. Introduction

It is common knowledge that unchecked urban expansion modifies ecosystems. The United Nations Member States partnership recently called for action for a better and sustainable future, adopting a list of 17 sustainable development goals (SDGs) about life on Earth, the environment, inequality, energy, and specifically the achievements of sustainable cities and communities (United Nations, 2015). Nevertheless, an over–simplified idea exists that nature–based solutions involve only the biotic compartment, and overlooks the role of the abiotic richness of Earth surface (Schrodt et al., 2019). When it comes to investigating the impact of human presence and activities on the environment, most of the literature focuses solely on changes in biodiversity (*e.g.*, Vačkář et al. (2012)).

Many scholars recently suggested that geodiversity is the geosphere counterpart of what biodiversity represents within the biosphere, atmosphere, and hydrosphere (Tukiainen et al., 2023), as geodiversity is "the natural range (diversity) of geological (rocks, minerals, fossils), geomorphological (land form,

Keywords: Geomorphometry, Geomorphodiversity, Land cover, Multiscale analysis, Urban geology

processes) and soil features" (Gray, 2008). The geosphere supports the natural processes occurring in the ecosystems and human health, through a wide range of ecosystem services (McDonald et al., 2018; Fox et al., 2020).

Since its introduction, several scholars studied geodiversity from the theoretical and practical points of view, with different approaches, assumptions and purposes (Zwoliński et al., 2018). Methods to define diversity of the geosphere are quantitative, qualitative, and hybrid approaches, with the occasional addition of heuristics, as described by Zwoliński et al. (2018) and references therein, and by Kubalíková and Coratza (2023).

Here, we approximate geodiversity through a quantitative derivation of geomorphodiversity index (GmI), representing the variety of features and the morpho–genetic processes modeling the landscape (Panizza, 2009), and lithological information (Benito-Calvo et al., 2009; Melelli et al., 2017; Burnelli et al., 2023).

We combine information of GmI with a newly developed quantity devoted to describing the degree of human impact on observed land cover classes, which we label as anthropization index, AzI. The latter is a reclassification of Copernicus' CORINE Land Cover (CLC; Feranec et al. (2016)) into ten new categories, inferred from the textual descriptions of the original CLC classes, and denoting increasing degree of anthropization. This differs form indices of anthropization existing in the literature, as they typically focus on the impact of human presence on the biotic components (*e.g.*, Lima Magalhães et al. (2015)). An existing map of anthropogenic impacts on the environment, the global human influence index (WCS and CIESIN, 2005), has much lower spatial resolution and it is not applicable, here.

The two indices considered here might suggest complementary information. Different classes of geomorphodiversity highlight the abundance and the variety of different landforms, as well as lithological, morphological and hydrographic variability and, as such, contain information about the degree of geomorphological activity (Howard, 1965; Leopold et al., 2020). Land surface and its diversity provide the abiotic framework and the resources for natural and human development. Land cover and land cover change give a measure of how these resources are exploited by the biosphere and by human activities. The anthropization index aims at distinguishing places with different degree of human impact.

Considering simultaneously GmI and AzI may allow us to define critical levels of human pressure and devise solutions, towards an increased sustainability of human impact on the landscape in urban areas, where the role of the abiotic component is often underestimated (Stewart and Gill, 2017).

We studied specifically GmI and AzI in Italy, consistently at relatively high resolution, with methods that one could readily apply elsewhere – above all in Europe, in which the same data used to define GmI and AzI is available. Specific objectives of this work are investigating (i) the relationship between GmI and AzI, (ii) the relationship between the two indices specifically in urban areas, consistently all over Italy and at high resolution, and (iii) the possibility of inferring implications of specific land cover changes scenarios, both for AzI and GmI spatial distributions.

As we are specifically interested in urban areas, we stress that their very definition is not unique. In fact, United Nations (2018) stated that *no standardized international criteria exist for determining the boundaries of a city and often multiple boundary definitions are available for any given city.* The definition of cities' administrative boundaries differ in different World countries. One relevant definition existing at global level is functional urban areas (FUAs), encompassing cities and their commuting influence zone obtained from statistical models. For example, Schiavina et al. (2022) recently studied land use efficiency within FUAs globally. Functional urban areas are also adopted in this work, to calculate statistics of the distribution of AzI and GmI values. We also used alternative definitions, not related to administrative boundaries but rather on indicators of human presence (Alvioli, 2020a,b), for comparison.

This paper is organized as follow. Next Section, 2, expands on the ideas of geodiversity, different possible scales of analysis and types of existing data, definition of landforms and of urban areas. Specific data used here are listed and described in Section 3. Section 4 illustrates in four sub–sections the approach to obtain geomorphodiversity and anthropization indices, and the assessment of their spatial distributions across Italy and specifically within different types of urban areas. Section 5 illustrates in detail the outcome of the analysis, including the implications of synthetic scenarios for land use change. Results are critically discussed in Section 6, and conclusions are drawn in Section 7.

2. Background

Urban geomorphology focuses on the changes to the natural landscape caused by human activities in cities (Thornbush and Allen, 2018). Human activities have been operating within cities in different times, causing modifications of the landscape that has an effect on natural processes, local diversity (Brandolini et al., 2020), and natural hazards (Sofia et al., 2017; Santangelo et al., 2021; Zumpano et al., 2021; Agrawal and Dixit, 2024). Urban geomorphology also analyzes resources in urban areas, including geoheritage (Reynard et al., 2017; Coratza and Hobléa, 2018; Pelfini et al., 2018).

Methods to quantify and map the impact of urbanization onto the landscape are mostly known and applied at fine scales, typically the scale of individual cities or urban agglomerations (Burnelli et al., 2024; Pica et al., 2024). These include both expert and objective methods, the latter requiring a wealth of high–resolution and multi–temporal data. Meter–scale elevation data, such as digital elevation models obtained from LiDAR and photogrammetry, allows one to delineate natural and anthropogenic landforms (Tarolli and Sofia, 2016; Vergari et al., 2022). This is useful for practical applications of urban planning by local administrations (Elmqvist et al., 2021).

At broad scales, where the focus is on agglomerations of cities or extended urban areas, completely different data sources are available. These are of different nature and exist at different (lower) resolution than data usually utilized for urban analysis and planning at individual city scale. Relevant examples are digital elevation models (DEM), land use, and land cover (LULC) data. In Europe, Copernicus obtains and publishes DEM and land cover data respectively at 25 m and 100 m resolution for all European Countries[1]. These are readily available to infer the distribution of landforms and land cover within urban boundaries and, possibly, their evolution in time.

High diversity at the local and regional scale and natural LULC have a positive feedback on the biosphere (Rahbek et al., 2019). Conversely, Rosa et al. (2024) recently showed that land used and modified by humans has lower functional richness, especially in croplands and urban areas, in different bio–regions and at large scale. This highlights that informed conservation strategies and sustainable land management across scales are needed, to reduce the impact of human activities onto biodiversity (Chakraborty and Gray, 2020).

From an analytic point of view, a meaningful and automated morphometric and morphological classification of land surface is more difficult than

[1]Available at https://doi.org/10.5270/ESA-c5d3d65

identifying individual landforms at one specific scale (Evans, 2012).

A specific landform has a recognizable pattern on the surface and an algorithm can single out any such pattern; the algorithm of Jasiewicz and Stepinski (2013) can distinguish up to 498 different ones, with a multi–scale method. Classification of any location of a given area into more generic categories be more challenging. For example, Hiwahashi and Yamazaki (2022) classified the whole globe into polygons of varying size and shape, distinguishing them with few morphometric features. For this reason, a consistent method for extracting landforms and their diversity across different geographical scales, which is accomplished with the GmI adopted here, improved from that of Burnelli et al. (2023), is of great importance.

Finally, we highlight that FUAs are administrative boundaries and, as such, do not necessarily reflect geomorphological properties and LULC classes within actual urban areas (Hamilton and Rae, 2020). In contrast, delineation of cities has been performed in a number of other different ways, relying on heterogeneous data sources and criteria, including: (a) population/urbanization density, (b) interactions, described by different kinds of networks, and (c) geographical proximity/contiguity (Masucci et al., 2015). Many such methods exhibit strong model or parameter dependence, for example on population or area thresholds.

One class of methods exist that considers landmarks of continued human presence as a basis for a parameter–free delineation of urban areas (Jiang and Liu, 2012). In particular, we consider here a delineation of urban areas in Italy (Alvioli, 2020a) built on the road junctions OpenStreetMap data (*e.g.*, Sarretta and Minghini (2021)). The dataset is a set of polygons exhibiting several kinds of scaling laws, which are relevant tools to study social, economic, and topographic properties of cities (Bettencourt et al., 2007; Cottineau et al., 2017). Most importantly, they follow an area–population scaling law comparable with that of European and World cities, obtained without fitting any parameter.

3. Materials

This work required the following input data:

- The Copernicus EU–DEM, a raster layer supplied by the European Environmental Agency (EEA)[2]. The horizontal resolution is 25 m and the vertical accuracy is of 2.9 m. Data is provided in the ETRS89-extended / Lambert Azimuthal Equal Area projected coordinate system (EPSG:3035). We converted all data used in this work in this coordinate system. Out of the European coverage of the data, we selected a bounding box covering Italy, in which elevation ranges between -60 m and 4,789 m.

- A lithological map of Italy at 1:100,000 scale, recently developed by Bucci et al. (2022)[3]. The map is distributed as a vector layer, in WGS84 geographical coordinates (EPSG:4326). The associated attribute table described 19 different lithological classes. Here, we are interested in diversity of classes, not the specific properties of each rock type.

- The CORINE Land Cover, available online from the Copernicus Land Monitoring Service[4] as raster data at 100 m spatial resolution. We used CLC for 1990, 2000, 2006, 2012, 2018. Data is distributed in the same coordinate system as EU–DEM.

[2]Available at https://www.eea.europa.eu/
[3]Available on the PANGAEA database: https://doi.org/10.1594/PANGAEA.935673
[4]Available at https://land.copernicus.eu

- Three different delineations of urban areas in Italy; two of them from the literature (Alvioli, 2020a,b)[5], and FUAs by the Italian Institute for statistics (ISTAT[6]).

The land surface diversity index GmI by Burnelli et al. (2023) is a quantitative measure of geomorphodiversity, obtained from lithological, morphological and hydrographic features. Geomorphodiversity is a proxy for geodiversity, it represents a key parameter for understanding the different morphological settings and, potentially, of the evolution of a landscape.

The published version of GmI has a spatial resolution of 500 m. In this work, we used the index at local and urban scale, which required a higher resolution raster map. The procedure to obtain the raster index required a few modifications of the original approach, and will be reported in Section 8. Inputs of the method to obtain the classified diversity map are three quantities derived from the DEM – namely slope, drainage density, and geomorphons Jasiewicz and Stepinski (2013), and a lithological map. Hence, the use of EU–DEM and the lithology at the highest geographical scale available to us, by Bucci et al. (2022).

CORINE land cover (CLC) is the well–known, open access set of land cover information for the whole of Europe, at 1:100,000 scale, with a minimum mapping unit of 25 ha and an accuracy better than 100 m. The 2018 version has a three–level classification, which identifies 44 land cover classes in the third level and 15 in the second level; the first level contains five classes: urban fabric, agricultural areas, forest and semi–natural areas, wetlands and water bodies. We explored the temporal dependence of the urbanization index defined in this work, using CLC raster maps for 1990, 2000, 2006, 2012

[5] Available at https://urgere-project.irpi.cnr.it/downloads/
[6] Available at https://www.istat.it

and 2018. Figure 1 shows the most recent release of CLC, and the original classes.

We considered different delineations of urban areas (UA), because it is widely acknowledged that the delineation of cities and urban boundaries depends on many factors, including input data, criteria to distinguish urban and internal areas, and purpose of the delineation. To take into account the uncertainty of definition of the UA, we considered three different datasets: (i) a parameter–free delineation based on indicators of "human presence", recently proposed by Alvioli (2020a); (ii) a more common definition based on a measure of terrain imperviousness (similar to 'paved areas', as discussed by Bettencourt (2013)), described in more detail by Alvioli (2020b); (iii) an official definition of FUAs, by the Italian Institute for Statistics, based on commuting zone information at municipality level.

We refer to these three different approximation as UA1, UA2 and UA3, respectively. We further distinguish FUAs (UA3) as "core" areas, $\mathrm{UA3}_{\mathrm{core}}$, and "extended", $\mathrm{UA3}_{\mathrm{ext}}$. The difference between core and extended FUAs in Italy is that the core (defined as City) correspond to the central municipality of each urban agglomeration, while the extended (defined as commuting zone) also includes the adjacent municipalities related to the central one by daily commuting fluxes. Figure 2 shows the geographical distribution of the different approximations, and Table 1 lists numerical figures about their size distributions.

4. Methods

We describe the methods adopted in this work in three separate paragraphs: the high resolution geomorphodiversity index, GmI in Section 4.1, the definition of AzI classes, in Section 4.2, the assessment of their geographical distribution, limited to urban areas, in Section 4.3; a direct comparison of the geomorphodiversity and anthropization indices, and an assessment of the geographical distribution of GmI values, in Section 4.4.

4.1. Definition of a geomorphodiversity index

We obtained a national GmI map of Italy following the method of Burnelli et al. (2023), with two main differences. First, Burnelli et al. (2023) obtained a GmI raster map at 500 m spatial resolution, downgraded from the spatial resolution of 25 m of elevation data from EU–DEM. Here, we obtained a GmI map at the same resolution of EU–DEM, suitable for the assessment of urban geodiversity within city boundaries, and for comparison/combination with CLC raster maps. Second, Burnelli et al. (2023) calculated partial diversity of four input quantities (slope, landforms, drainage density, and lithology) with a circular moving window (or focal statistics analysis) of fixed radius. Here, we introduced a scale–independent methods which considers contributions of partial diversities calculated with a range of radii.

Figure 3 shows the workflow adopted in this work to obtain a national, scale–independent GmI map at high resolution. We used the same input quantities used by Burnelli et al. (2023): (1) slope angle, calculated EU–DEM with the default GRASS GIS (Neteler and Mitasova, 2008) (version 8.3) algorithm; (2) ten landform classes, obtained by the geomorphons classification method, based on recognition of ten different pre-defined patterns: flat, peak, ridge, shoulder, spur, slope, hollow, foot slope, valley, and pit (Jasiewicz and Stepinski, 2013); (3) 19 lithological classes, from the 1:100,000 map by Bucci et al. (2022); (4) a drainage density obtained by a neighborhood analysis of the river network obtained from the European Union's Earth observation programme Copernicus[7]

[7]https://www.copernicus.eu

The algorithm to obtain the national GmI map consists of three main steps. First, selecting a range of sizes (or radii, R_i in Fig. 3) for moving windows to calculate partial diversity maps of the four input quantities. Second, obtaining partial maps running the `r.neighbors` module in GRASS GIS, with the "variety" statistics, for each selected value of the radius. Third, classifying each partial diversity raster map in five categories using Jenks breaks, combine (sum) the four map corresponding to the same value of the radius, and classify again into the five final GmI classes. Five, dropping the parameter dependence (effectively scale dependence) by combining the set of radius–dependent GmI maps into a single map, selecting for each cell the most common value across the set of maps.

We highlight, here, that we combined the four partial diversity maps considering them on the same footing, by classifying their variety into the same number of classes (five) – to combine them into a single index, GmI. As in Burnelli et al. (2023), inclusion of drainage density was dictated by the aim of calculating an index on the entirety of the Italian peninsula. Considering slope, geomorphons and lithology alone would produce a trivial result in plain areas – for slope is in the lowest class everywhere, lithology is "alluvial" and geomorphons class is "flat". We acknowledge that there may be alternative approaches to the use of drainage density but we also believe that in this work, at national scale, it provides a reasonable approximation to distinguishing different zones in flat areas. Moreover, we stress that sum of classified rasters is the simplest choice to combine the four partial diversity map (slope, landforms, lithology, drainage density) obtained from the "moving windows" approach. The combination of moving window/sum of parameters fall within the most used methods for the assessment of geodiversity outlined by Zwoliński et al. (2018), *i.e.*, the use of geodiversity indices and map algebra techniques.

We end up with a classified raster GmI that includes contributions from spatial neighborhood ranging from 275 m (11 grid cells, at 25 m spatial resolution) to 2,275 m (91 grid cells). We consider this raster map as a multi–scale geomorphodiversity index of Italy, which we deem as a good approximation to the variety of geomorphological features, obtained in an indirect way -– using only morphometric and lithological information, as field–based geomorphological maps do not exist for such a large area. Figure 4 shows a national map of the index, with two insets showing details in selected areas and the distribution of elevation, within each class. The original and updated maps are available for download (see Section 8).

4.2. Definition of an anthropization index

We defined an AzI of Italy, based on reclassification of CLC information, inferring the degree of human modifications from the legend of the original CLC data.

The classification is new to this work, and it describes increasing levels of human impact. The motivation for a new index stems from the need of quantifying anthropic impacts independently from the delineation of urban areas, which (i) is model dependent, and (ii) it only describes urban *vs.* non–urban areas, in any of the three definitions adopted in this work. The AzI contains ten classes, with increasing level of human impact on the landscape, listed in Table 2. The table includes the CLC classes and codes included in each new AzI class, with codes matching those in Fig. 1, as well as a synthetic summary of CLC names.

In the newly defined index, Class 1 includes the CLC classes “wetlands” and the “open space with little or no vegetation”, which were easily understood as the least affected by human activities. Class 2 includes “standing forests", with different degrees of forestry management, but keeping a large role in bio-conservation. Class 3 includes "transitional woodland and shrub", "heathland, sclerophyllous vegetation" and "burnt areas"; these are mixed and transitional zones, impacted by reforestation and/or similar external activities. Class 4 corresponds to "natural grasslands", class 5 to "pastures", characterized by a constant human and livestock presence, which impacts plant growth and selection of species. Class 6 includes "marine waters", different from class 7, which includes "water bodies" and "water courses", since the latter are significantly affected by human modifications as compared to coastal lagoons and estuaries, classified as "water bodies" in the CLC dataset. In class 8 we included all the CLC parcels falling into the "mosaic farmlands" group: here, the high level of anthropization coexists with a good variability on the biotic level. The classes 9 and 10 of the AzI refers to the "arable land and permanent crops" and to the "artificial surfaces", respectively.

Figure 5 shows the results for the national map, with ten AzI classes corresponding to the 2018 CLC release, and the distribution of elevation within each class. We obtained a temporal dependence of AzI corresponding to the reclassification of five different CLC releases spanning 1990–2018. Table 3 shows the variation of percentage coverage for each release. The classified AzI map is available for download (see Section 8).

4.3. Anthropization in urban areas

We studied the distribution of AzI values within the three definitions of UA adopted here, namely UA1, UA2 and UA3$_{\mathrm{ext}}$. We disregarded UA3$_{\mathrm{core}}$ because they are a subset of UA3$_{\mathrm{ext}}$, with substantially smaller spatial extent (*cf.* Table 1 and Fig. 2), and we deem the analysis within the smaller area less significant.

For each UA set, we labeled individual polygons according to their size, distinguishing small, large and very large UAs. A head/tail procedure gave the classification based on size. It works iteratively, calculating the mean size of the dataset that acts as a threshold for "small" areas. Calculating the mean of the remaining features in the dataset further distinguishes "large" and "very large" sizes. Table 1 lists the first threshold (overall mean) for each UA dataset. The head/tail split is particularly effective for UA1 and UA2, containing thousands of polygons with a size distribution very skewed towards small areas. Any other way of splitting size–wise would produce numerically very imbalanced subsets. The method is also suitable for splitting UA3.

In addition, we investigated the distribution of AzI classes considering their geographical location, distinguishing Southern, Central and Northern Italy, using the official definitions (see Fig. 2(c)).

Figure 6 shows results in six different sets of histograms, where size and location are distinguished. The histograms are discussed in the Section 5.

4.4. Combining geomorphodiversity and anthropization indices

The GmI has a resolution of 25 m, whereas the AzI is available as a 100 m raster map. For a direct comparison of the two maps we worked at the highest resolution (25 m), and calculated the percentage of grid cells for each combination of the five classes of GmI versus the ten classes of AzI. Figure 7 shows results of the calculations with a *heatmap*. Each rectangle in the figure is colorized with a green–to–blue ramp, describing increasing percentages of overlap.

Next, we investigated the distribution of the GmI values within urban areas, in the same way as we did for the AzI index described above, *i.e.*, distinguishing the size and location of UAs. Results are in Fig. 8.

Finally, we suggest a joint visualization of GmI and AzI distributions, adopted in Fig. 9. That is easily done assigning a color code to each of the 50 possible combination of the two indices (five GmI classes, *vs.* ten AzI classes). In the figure, the legend shows a four–fold color ramp used to colorize the various combinations in the maps. Figure 9 shows UAs containing the cities of Forlì—Cesena, Genoa and Milan, in Northern Italy; Pisa, Perugia and Rome, in Central Italy; Taranto, Naples and Palermo, in the South. Each triplet contains a small, a large and a very large UA, according to the split of $\mathrm{UA3_{ext}}$ sizes adopted here, which are shown as thick black contours. Each figure also shows boundaries of UA1, shown as thin black polygons, filled with a dotted pattern. One can see the substantial difference between these two different ways of referring to UAs, in the nine sample areas considered in the figure. Note that the scale in the different panels is either 1:275,000 or 1:500,000; details are in figure's captions.

The combined GmI–AzI map and legend are available for download (see Section 8).

To propose a sample application of the two maps discussed in this work, we devised a few scenarios for land cover change, studying the implications for the AzI and GmI maps. We hypothesized scenarios in which either artificial surfaces, or arable land and permanent crops, or simultaneous both land covers expand. These correspond to AzI = 10 and AzI = 9, respectively – the highest and second highest classes of anthropization. We devised scenarios as follows.

Scenario 1 (S1): expansion of AzI = 10 class, to simulate an expansion of urban fabric and loss of adjacent land cover types; we constrained the expansion to very large clusters of AzI = 10 contiguous cells (selected with the head–tail break criterion used previously). We let such clusters expand by one 25 m grid cell in every direction. Scenario 2 (S2): as in S1, but expanding the large cluster of artificial surfaces by two grid cells in every direction. In S1 and S2, we took care of keeping fixed the AzI classes corresponding to water bodies and courses.

Scenarios 3 and 4 (S3 and S4): as in S1 and S2, but expanding the AzI = 9 class by either one or two grid cells in every direction. This simulates an expansion of temporary and permanent crops, and loss of adjacent land cover classes. In these scenarios, in addition to water courses (AzI=6, 7), we also kept unchanged the AzI = 10 class.

Scenarios 5 and 6: a combination of S1 and S3, and of S2 and S4, respectively. The results are scenarios in which artificial surfaces, temporary and permanent crops are expanded simultaneously, either by one grid cell (S5), and by two grid cells (S6), in every direction. In the process, in addition to keeping fixed the AzI=6, 7 classes, we did not let the AzI = 9 overwrite the AzI = 10 grid cells.

Results of land cover changes S1–S6 are in Table 4. The table is split into results within each scenario for what concerns the modified AzI maps, and their relationship GmI map.

Although the slope angle appears to be the determining factor in the distribution of the GmI classes, in reality all the factors taken into account have an equal weight. The relationship with slope angle is due to the fact that the Italian territory is geodynamically active and there is a close correlation between structural factors and geomorphological evolution. This makes the interpretation of the geomorphic diversity even more valid, taking as input factors those considered in this study.

5. Results

5.1. High–resolution geomorphodiversity index

The new GmI map of Italy, obtained in this work, is shown in Fig. 4. The main figure shows the national map, two insets zooms into selected areas, and violin plots with the distribution of elevation, within each class. Violin plots in Fig. 4 indicate that class 1 (very low GmI) is limited to altitudes below 1,000 m. This is understood considering that class 1 is mostly present in the Po Valley, which has altitudes between 0 and 200 m. Areas with GmI = 2 are also limited to lower altitudes, to a smaller degree. Class GmI = 3 shows the most homogeneous distribution. Class 4 is mostly represented at lower altitudes, but also extends to the highest altitudes, similarly to class 5 (although less abundant under 1 km a.s.l.). In both cases, the high GmI values at lower altitudes are related to the use of drainage density as one of the inputs to obtain the final GmI. In fact the most important floodplains in Italy are close to the coastline or, for the highest elevation values, the highest Alpine and Apennine peaks, with large slopes. Slope angle is one relevant input factor in the definition of GmI.

5.2. Distribution of anthropization index values

Figure 5 shows the map of the anthropization index, defined in this work as described in Section 4, and prepared with the 2018 release of CLC. For each class, an overview of the distributions of elevation values is also given. Table 2 lists the percentage coverage of each AzI class. Figure 5 correspond to the 2018 release, while the table reports result for five CLC maps, corresponding to five releases, spanning 1990–2018.

The most widespread class (AzI = 9, arable land and permanent crops), the second largest class (AzI = 2, standing forest) and the third (AzI = 8, mosaic farmland) cover overall more than 75 % of Italy.

Class AzI = 9 corresponds to areas with a relevant human impact and is mostly located in lowlands, as we can clearly see in Fig. 8. It is often characterized by modified rivers or channels, mostly embedding areas with AzI = 10 (artificial surfaces). Class AzI = 9 decreased in the time span considered in Table 2, while class AzI = 10 increased (corresponding to expansion of the urban fabric); their sum slightly increased.

Areas with AzI = 1, 2, 3 (and 4) are associated with more pristine natural environment, they cover overall 124,380 km^2, about 42 % of Italy. Class AzI = 5 cover just 1.38 % and decreased slightly.

Class AzI = 2 (standing forests) extends mostly along major valleys in the Alps, and less in the Apennine and Peninsular parts. This class extends from low elevations to about 2,000 m, with the majority between about 500 m and 1,000 m (*cf.* Fig. 8). The percentage coverage seems to have remained constant across the last 30 years.

Values of AzI = 6, 7 corresponding to marine waters, water bodies and water courses cover overall less than 1 % and did not change in time. Water courses, artificial rivers and canalised channels fall into these categories and are mainly distributed along the Po river valley and the coasts.

Class AzI = 8 is characterized by substantial human impact in hilly or flat areas and valleys, with sparse buildings in low elevation areas, but it does not contain permanent crops. The percentage coverage of this class did not change substantially in the considered time period.

Figure 6 shows the distribution of the AzI values within the three urban boundaries considered in this work. The figure compares the distributions in UAs of different sizes (panels on the left column) and with different geographical location (right column). Size of UAs are distinguished by small (smaller than average, in each UA definition), large (larger than average) and very large (larger than the average large areas); the geographical distributions distinguishes UAs in Northern, Central and Southern Italy, shown in Fig. 2(d).

In all of the panels of Fig. 6, for each AzI class, we reported the national percentage coverage (horizontal dashed lines), for comparison with the corresponding value within urban areas. It is straightforward to observe that the classes AzI = 2, 8, 9 and 10 are the most relevant ones, in UAs, which is not the case for the national distributions. Class AzI = 10 is above the national value, which is expected in urban areas, given that it represents areas with highest human impact. Considering the extended functional urban areas (corresponding to a clustering of administrative boundaries), the last consideration can be extended to classes AzI = 8, 9 and 10, regardless of the size or the location of the areas. That does not hold true for UA1 and UA2, as the frequency in class AzI = 9 is always lower than the reference value, while class AzI = 10 is several times larger. This is not surprising, as both delineations of urban areas (using indicators of continued human presence, in UA1, and impervious/paved ground, in UA2) extend further than the built–up regions but do not artificially include substantial parts of internal areas. Municipal boundaries in $\mathrm{UA3}_{\mathrm{ext}}$ include parts of internal areas, thus the distribution of AzI values within these boundaries are very close to the national reference values.

A relevant difference between UA1, UA2 and $\mathrm{UA3}_{\mathrm{ext}}$ is that UA1 and UA2 contains a large number of very small areas; *cf.* Table 2. In the case of UA1, this is due to the Delaunay triangulation algorithm used to delineate the areas starting from road junctions, while in the case of UA2 the smaller area is 400 m^2 and it corresponds to one grid cell of the original 20 m raster resolution. Both UA1 and UA2 were designed to reproduce an area–population scaling law (Alvioli, 2020a,b), which breaks if one artificially removes areas within a particular range in size. Thus, we kept the full vector layer datasets of UA1 and UA2, here.

The total area of small areas (*i.e.*, smaller than the average in each dataset) in is 11 % in UA1, and 21 % in UA2. Figure 6 shows that, in the most relevant classes (AzI = 8, 9 and 10), small areas (green bars) have a different tendency than large ones (red bars), as they contains a larger fraction of AzI = 8, 9 values and a smaller fraction of AzI = 10 values. This is much more pronounced for UA2 then UA1.

The anthropization index in UAs does not show a strong dependence on geographical distribution (panel on the right column in Fig. 6), as the bars corresponding to all three versions of UAs show similar behavior in the three cases. One difference is that, for UA1, urban areas in Southern Italy contain more AzI = 8, 9 values and less AzI = 10 values, whereas the most natural land use, AzI = 1 to 5, are more abundant in smallest and Southern cities. The observed frequency in AzI = 10 means that UA1 are more similar to the standard CLC artificial surfaces in Northern and Central Italy, and less in the south. This class includes industrial activities, buildings and artificial non-agricultural vegetated areas (leisure sites, green parks, etc). This is not true for UA2, which is understood considering that artificial surfaces largely correspond to the impervious areas used to single out polygons in UA2.

5.3. Distribution of geomorphodiversity and combined indices

Next, we investigated the relationship between the geomorphodiversity index of Burnelli et al. (2023) and the anthropization index obtained here. Figure 7 shows a heat map obtained from the percentage coverage of each GmI–AzI value combination. The general trend shown by the figure is easily understood, as the two peaks correspond either to high GmI–low AzI, and vice–versa. Negligible percentages corresponding to AzI = 6 and 7, for any value of GmI, are simply due to the small coverage of the two classes (0.06 % and 3.5 %, respectively). In a similar way, the peak at low values of GmI and large AzI is found for AzI = 9 instead of AzI = 10 because class 9 covers altogether 47 % of Italy, while class 10 covers only 5 % (*cf.* Fig. 5).

Next, we present results for the distribution of land surface diversity, GmI values, within urban areas. We prepared histograms for GmI distributions in a similar way to the AzI case, shown in Fig. 8. At variance with the AzI distributions, results are more uniform across the different UAs definitions.

The left panels show that the lowest and second–lowest percentages of land surface diversity within UAs are larger than the corresponding national averages, while values of GmI ≥ 3 are smaller. In this respect, the results for UA1 and $\mathrm{UA3_{ext}}$ are more similar. More in detail, results for UA1 and UA2 show that very large (VL, in the figure) cities have slightly lower percentages than large and small cities, for GmI ≥ 3; the case of $\mathrm{UA3_{ext}}$ show the opposite trend.

The right panels have similar patterns; percentages are higher than the reference values for GmI ≤ 2, and lower than reference for GmI ≥ 3, for all UAs variations. The largest deviations from the national values are for GmI = 1, mostly due to UAs in Northern Italy, while UAs in the center and south are mostly aligned with the reference. Values of $2 \leq$ GmI ≤ 4 are more represented in UAs in Central and Southern Italy. Moreover, UAs in Central Italy show larger land surface diversity than in Southern and Northern Italy. The areas with largest values of land surface diversity, GmI = 5, are much lower than the national values, for all UA variations and across Italy, except for UA1 in Northern Italy.

Figure 9 shows a joint graphical representation of GmI and AzI classes, within three sample of urban areas in the Northern, Central and Southern Italy, respectively (nine examples in total). For each geographical domain, we included on example of small, large and very large UAs, considering the extended FUAs size classification (size of $UA3_{ext}$; *cf.* Table 2 and Fig. 4).

In all of the considered locations, $UA3_{ext}$ boundaries substantially exceeds the cities' core as delineated by UA1, and each $UA3_{ext}$ polygon contains several disjoint AU1 areas. The UA1 polygons are usually closer to high AzI values (brown–ish to white–ish areas), with a variable mixture of GmI values. This is understood considering that the definition of large AzI values explicitly contains artificial surfaces, and GmI values are distinguished according to the underlying topography and lithological information.

These general findings have variations within the different settings of Fig. 9. Low–AzI city cores are mostly embedded low–GmI regions in the case of Forlì–Cesena and Milan, Figs. 9(a) and (c), Pisa, Fig. 9(d), and Taranto, Fig. 9(h). The same holds to a lesser degree in the case of Perugia, Fig. 9(e), and Naples, Fig. 9(i).

The cities of Genoa, Rome and Palermo, Figs. 9(b), 9(f) and 9(i), instead, show much larger values of GmI, especially in Genoa and Palermo, in which the city core is markedly characterized by intermediate– to large–AzI and large–GmI values, and surrounded by large GmI and lower AzI, in the extended FUAs. This is due to the proximity of high relief areas, in the case of Genoa. In general, extended FUAs show varying distributions of GmI–AzI combinations. To comparatively understand these distributions, one must consider the actual sizes of the regions shown in the panels, as we used different scales.

5.4. Land cover change scenarios

As we stressed, one crucial difference between the AzI and GmI maps presented here is the different rate of change with time, as AzI rate of change may be of a few years. GmI can be considered constant over this time scale, at least in absence of artificial, local changes. One possible joint application of the AzI and GmI maps is studying different scenarios for land cover change and the values of GmI in the modified areas. Section 4.4 defined a few change scenarios, in which we let temporary and permanent crops (AzI=9), artificial surfaces (AzI=10), or both simultaneously, expand from the percentages coverage listed in Table 3 (column 2018). The results of this exercise are in (Table 4).

The top half of Table 4 shows the relative modifications of percentage coverage of each AzI class, for each scenario, S1–S6. Column '2018' corresponds to percentages the original AzI map. Columns S1, S2 (scenarios that simulate expansion of artificial surfaces, with different extent) causes smaller loss of coverage in AzI = 1, 2, and larger loss in AzI = 8, 9 classes. This is easily understood considering that artificial surfaces are mostly adjacent to arable lands, permanent crops, and mosaic farmlands. Columns S3, S4 (scenarios for expansion of arable land and permanent crops), instead, causes loss of most of the AzI classes; only water bodies and artificial surfaces are constant, by construction. Columns S5, S6 are a combination of the first two kinds of scenarios (*i.e.*, both AzI = 9 and AzI = 10 were allowed to expand), and the numerical results are consistent with a combination of the results in columns S1–S4. Specific differences between percentages in different scenarios are function of the spatial distribution of AzI classes with respect to those that were allowed to expand.

The bottom half of Table 4 aims at showing the geodiversity classes involved in the land cover changes implied by the six artificial scenarios. The values listed in the table are the percentages of each GmI class limited to the grid cells that switched AzI class, as a consequence of scenario changes. The values in column S1 show that when artificial surfaces expand, these mostly affect low values of GmI; the percentage decrease for increasing value of GmI. Values in column S2 are similar; we note that with increasing area of change in AzI = 10, as in S2 with respect to S1, larger values of GmI are slightly more affected. The values in columns S3–S6 have a substantially different tendency, in that the largest values correspond to GmI = 3, and higher values of GmI are equally affected than lower ones. Absolute values are slightly smaller in S5 and S6 (change in both AzI = 9 and AzI = 10), consistently with the results in S1–S3, and S2–S4.

These sample results are obtained from synthetic scenarios, where change were applied with general criteria, all over Italy. Specific results may be obtained with realistic projections of land cover change and, possibly, constraints dictated by topography or other quantitative arguments.

6. Discussion

A few authors used additional quantities in their definitions of geomorphodiversity, with respect to that of Burnelli et al. (2023) adopted here, which includes slope, drainage density, lithology, and subset of terrain landforms. For example, Benito-Calvo et al. (2009) and (Melelli et al., 2017) used did not explicitly use landforms. In general, one can argue that many other variables from the geology, geomorphology, hydrology and pedology sectors are useful variables to define geomorphodiversity or, more in general, geodiversity.

Nevertheless, we believe that the efficacy of a model is not contingent upon the multitude of input variables, but rather upon the minimal set of variables that reproduce the essentials of a natural phenomenon. The factors considered in GmI encompass both the structural factors and the modeling agents responsible for shaping the existing landforms. Here, we used a minimal set of publicly available input data, and applied a clear, reproducible, and objective method to process them and obtain indicators of land surface diversity and anthropic impact on land use. This reduces model dependency to a minimum, and make results as robust as possible.

The climatic factor is one relevant piece of information that was neglected, here. Climate contributes to the formation of a landform and its evolution over time, as it can significantly alter the morphometric and evolutionary characteristics of a morphotype. We postponed climatic zonation to a later analysis in order to obtain results based primarily on topographic variables.

Simplicity of the approach makes the definition of geomorphodiversity adopted here readily applicable at continental or global scale, as the necessary data is available worldwide with comparable quality and resolution. That is elevation data and river networks, either from independent cartography or delineated on the digital topography. Lithology/geology information used by Burnelli et al. (2023) was available at relatively high resolution (1:100,000, Bucci et al. (2022)). Global geology maps, for example, GLiM v1.0 (Hartmann and Moosdorf, 2012) has considerably lower spatial resolution, and using it in would imply a lower resolution of the final GmI.

The information contained in the AzI map, new to this work, conveys in a simple and intuitive way the degree of human influence, inferred from the definitions provided with the original CLC classes (refer to Table 2). We suggested that the joint study of GmI and AzI within polygons delimiting urban areas is meaningful.

We note that the use of independent urban boundaries may appear redundant with class AzI = 10, as this class is defined by "artificial surfaces".

In reality, only one of the three definition of urban boundaries adopted here (UAs) has similar meaning to artificial surfaces, namely, UA2. The latter is based on a measure of terrain imperviousness (*i.e.*, the degree of sealing), and they probably correlate with artificial surfaces. On the other hand, UA1 and $\mathrm{UA3}_{\mathrm{ext}}$ differ substantially.

We stress that analysis of individual urban areas should be supported by more detailed analyses, using additional information and combining multidisciplinary methods. Knowledge of the historical evolution and the anthropic variables that have conditioned the urban development of a city over the centuries, especially for those with ancient foundations, is key to understanding the evolution of abiotic variables in the urban fabric. Moreover, anthropogenic transformations can distort the topographic response and the spatialization of land use, which calls for a historical analysis. The Italian territory remained fragmented for centuries and was only recently unified (second half of the 19th century). The type of anthropic settlement is also a consequence of the policies adopted in the different areas over the centuries. In short, a comparison with other disciplines and the consideration of variables for detailed analyses would be desirable.

The results presented in Fig. 4, for the GmI map, in Fig. 5, for the newly developed AzI, and Figs. 6–9, for the relationship between AzI, GmI and urban areas in Italy, can be understood with general considerations about the morphological settings in Italy (Marchetti et al., 2017). Italian lowlands, where the GmI has low values, features dense urban settlements, whose extent is constant comparing the different CLC through time (*cf.* Table 3). Figure 9 clearly show that a less diverse territory, mostly characterized by alluvial plains, or gently hilly zone, was used for urbanization and agricultural activities such as permanent cultivations (AzI = 9, 10). Projections of urban expansion indicate a "slope climbing trend" of cities (Shi et al., 2023), meaning that urban growth is expected to shift from flat areas to higher slopes and altitudes. This has implications for natural habitats, including forests and grasslands; the relevance of this effect specifically in Italy should be investigated more in detail.

Conversely, the most natural environments (AzI = 1–4) are dominant along the Alps and Apennines mountain chains, with a rough surface, where scattered urban settlements exist. A complex landscape results in high land surface diversity, where terrain dynamics and surface processes do not foster the city development and expansion.

Where intermediate GmI values exist, the most frequent land cover is a mosaic farmland (AzI = 8). Here, human signatures are sparse, and represented by fruit orchards, olives, pastures, and scattered houses or gardens. The landscape is characterized by landforms of different sizes, and elevation ranges between a few hundred to 1,000 m (*cf.* Fig. 5). This class does not change over time, which may be explained by the environmental peculiarities of these terrains, which discourage human activities.

The examples considered in Fig. 9 somewhat indicate that the smallest UA in each group shows larger levels of anthropization and small geomorphodiversity. This is largely due to the topography of the three examples. Forlì–Cesena is located between the Appennine chain and the Po plain, where the elevation ranges between 0 and 500 m a.s.l. (see Fig. 4), and the vast majority of the flat area is urbanized, whereas the highest degree of naturalness and geodiversity are found near the Appennine. The area of Pisa and Taranto mostly includes plain areas as well, near the coast, in Tuscany and Apulia.

A less marked pattern in the considered examples is that two of the three largest areas in each group, Rome and Palermo, Figs. 9(f) and 9(i), show medium–high GmI even in the areas bounded by UA1 polygons, and areas with both high GmI and low AzI in the surroundings. On the other hand, in the case of Milan, Fig. 9(c), the 'very large' city in Northern Italy which extends in the Po plain, the discussion is similar to the three cases of small UAs: it is a flat area, highly urbanized in many respects, including built–up areas and modified water courses.

In general, the high–resolution combined indices description of urban areas allows to single out specific topographic features, and put the into the perspective of GmI and AzI values. For example in Forlì—Cesena (Fig. 9(a)), the combined map shows the sharp change between Central Apennine chain and the southern portion of the Po plains, with several scattered areas with low GmI and/or large AzI on the non–flat areas. In Milan (Fig. 9(c)), one can see the paths of Ticino and Adda rivers, on the western and north–eastern sides respectively, generating hot–spots of larger GmI with respect to the surrounding areas, and the sudden change between the flat area and the Alps in the north.

Figure 9 also graphically highlights the differences between urban boundaries by Alvioli (2020a), UA1, and functional urban areas, $UA3_{ext}$, thus the different role they may play in the context of spatial analysis and environmental planning. In all figures, UA1 represent the regions where actual human presence is inferred, at variance with $UA3_{ext}$, corresponding to administrative boundaries. This means that while the former may be more suitable for an assessment of the relationship between land cover and the geographical location of cities, the latter are the boundaries in which actual planning decisions have an effect, and resources are allocated.

Figure 9 aims at showing examples of the application of a combined GmI–

AzI distribution. We maintain that the combination of the two indices is meaningful, because the first index contains land surface information that remain constant in relatively short time intervals, while the CLC data used to define the second index is sampled at four years intervals. Thus, in principle, one can prepare different versions of GmI–AzI indices only replacing the AzI information. Studying the time dependence of the definition of city boundaries instead, though equally interesting, require spatially distributed data that is not available to us.

Table 4 lists the relative change of anthropization classes as a consequence of synthetic scenarios for land use change. They represent a hypothetical application of the index introduced here, and provide information on the geomorphodiversity classes affected in each scenario. We stress that the scenarios were arbitrary, but we maintain that they give insight into the GmI–AzI combination.

7. Conclusions

The role of geomorphology in the urban environment can benefit from quantitative analyses summarized with concise indices that can be easily reproduced in different geographical contexts. For example, in identification of geoheritage, they can highlight morphological conformations with a strong propensity for naturalness. In these cases they provide an objective analysis that goes beyond the logic of territorial administration, which are very often influenced by motivations that cannot be traced back to territorial reality. Furthermore, spatial indices can be used for multiscalar and multitemporal models and thus represent an important line of research for analyzing the temporal variability of geodiversity.

We defined an anthropization index, AzI, with a simple reclassification of CLC classes, to examine its relationship with the land surface diversity index, GmI, and to investigate the potential implications of increasing levels of human impact on the landscape. We considered particularly relevant the joint study AzI and GmI within urban areas, as they contain different information at different rates of change in time.

We have marginally investigated the temporal evolution of AzI, considering multiple CLC datasets, spanning 1990–2018. The most significant temporal variation of the Italian land use pertains to natural areas, like open spaces and natural grassland, and artificial surfaces. Moreover, we simulated a few land cover change scenarios, showing the amount by which classes in AzI and GmI that would be affected by the expansion of anthropized areas (classes AzI=9 and AzI=10).

The outcomes allow us to draw the following conclusions:

- Study of the spatial arrangement of abiotic parameters in urban areas is possible with high detail, using public datasets, considering the complementary information contained in the GmI and AzI raster maps proposed here.

- To study the effects of human pressure on the environment, it is crucial to distinguish artificial urban boundaries from boundaries denoting actual human presence and their activities. Statistics of GmI, AzI, and their relationship differ substantially, within different urban delineations.

- Synthetic scenarios of land use change, corresponding to different values of anthropization, are useful to study the effect on areas with different values of geomorphodiversity.

These conclusions show that a quantitative study of geomorphodiversity may represent an additional tool in the Earth Sciences to investigate the landscape variability in urban areas and, possibly, their inherent relationship between geodiversity and biodiversity. They provide knowledge regarding the influence of land use/land cover and the variability of landforms, which may help a sustainable planning in the development of urban areas.

8. Data availability

Results of this work are maps of (i) a new geomorphodiversity index map, calculated at 25 m consistently over Italy; (ii) 10 classes of the anthropization index AzI, Fig. 5, and (iii) 50 combined classes of GmI *vs.* AzI, Fig. 9. Both are available for download at the main website of the project URGERE, `https://urgere-project.irpi.cnr.it/`. Maps are in the reference system of EU–DEM, namely ETRS89-extended / LAEA Europe EPSG:3035, and have 25 m resolution. The map of GmI at the same resolution is also available. Any other intermediate result is available upon reasonable request.

9. Acknowledgments

Research supported by Project "URGERE: URban Geodiversity for a Resilient Environment" 2022M7EP3M_PE10_PRIN2022 - PNRR M4.C2.1.1 - Funded by the European Union – Next Generation EU - CUP: B53D23007260006.

We are grateful to Federico Fugnoli (CNR IRPI), Perugia, for the preparation and maintenance of the project website.

UA model (source)	**Min area**	**Max area**	**Mean area**	**Total area**	**No. of areas**	**No. small**	**No. large**	**No. very large**
	[m^2]	[km^2]	[km^2]	[km^2]	–	–	–	–
UA1 (Alvioli, 2020a)	0.01	1,311	0.24	21,073	89,272	79,945	7,930	1,397
UA2 (Alvioli, 2020b)	400	444	0.21	13,899	66,654	58,130	7,031	1,493
	[km^2]	[km^2]	[km^2]	[km^2]	–	–	–	–
$UA3_{core}$ (ISTAT)	30	1,327	203	16,851	83	51	18	14
$UA3_{ext}$ (ISTAT)	59	6,156	773	64,189	83	53	22	8

Table 1: Size characteristics of the different urban boundaries considered in this work (see Section 3). The distinction in small, large and very large is described in Section 4.2.

AzI	Percent area	CORINE Land Cover class names	CORINE codes	CORINE classes
1	5.34	Wetlands	4.*	35–39
		Open space with little or no vegetation	3.3.*	30–32, 34
2	26.42	Standing forests	3.1.*	23–25
3	7.21	Transitional woodland and shrub	3.2.4	29
		Heathland, sclerophyllous vegetation	3.2.2-3	27, 28
		Burnt areas	3.3.4	33
4	2.54	Natural grassland	3.2.1	26
5	1.38	Pastures	2.3.1	18
6	0.20	Marine waters	5.2.*	42–44
7	0.74	Water bodies	5.1.2	41
		Water courses	5.1.1	40
8	15.00	Mosaic farmlands	2.4.2-4	20–22
9	35.75	Arable land and permanent crops	2.1.*, 2.2.*, 2.4.1	12–17, 19
10	5.42	Artificial surfaces	1.*	1-11

Table 2: Lookup table between AzI and CLC names, codes, and classes; the latter correspond to the legend in Fig. 1. Asterisks in the column "CORINE code" mark either any third level class, or any second and third level class, falling within the same row in column "CORINE class name". We also list the percent area covered by each class.

Anthropization index (AzI)	**CORINE Land Cover (year, %)**				
	1990	2000	2006	2012	2018
1	3.81	3.42	3.18	5.32	5.34
2	26.07	26.20	26.50	26.45	26.42
3	7.40	7.33	7.26	7.20	7.22
4	4.83	4.89	4.60	2.56	2.54
5	1.52	1.42	1.43	1.38	1.38
6	0.19	0.19	0.19	0.19	0.20
7	0.72	0.73	0.73	0.74	0.74
8	14.57	14.61	14.93	15.00	15.00
9	36.50	36.43	36.07	35.77	35.74
10	4.39	4.72	5.12	5.38	5.42

Table 3: The temporal variation of the anthropization index (AzI) classes considering the CORINE Land Cover classification for 1990, 2000, 2006, 2012 and 2018.

Anthropization index (AzI)	**2018**	**S1**	**S2**	**S3**	**S4**	**S5**	**S6**
1	5.34	5.33	5.33	5.27	5.21	5.27	5.21
2	26.42	26.40	26.38	25.83	25.30	25.81	25.26
3	7.21	7.21	7.20	7.03	6.86	7.03	6.85
4	2.54	2.54	2.54	2.50	2.47	2.50	2.47
5	1.38	1.37	1.37	1.34	1.31	1.34	1.30
6	0.20	0.20	0.20	0.20	0.20	0.20	0.20
7	0.74	0.74	0.74	0.74	0.74	0.74	0.74
8	15.00	14.92	14.85	14.22	13.52	14.15	13.37
9	35.75	35.63	35.51	37.43	38.96	37.31	38.73
10	5.42	5.66	5.87	5.42	5.42	5.66	5.87

Geomorphodiversity index (GmI)	**S1**	**S2**	**S3**	**S4**	**S5**	**S6**
1	33.52	33.50	10.86	10.84	13.63	13.60
2	28.08	28.04	20.96	20.91	21.83	21.78
3	17.14	17.14	31.49	31.45	29.74	29.71
4	13.44	13.45	25.86	25.89	24.34	24.37
5	7.82	7.87	10.83	10.91	10.46	10.54

Table 4: Results for different scenarios of AzI change, for the AzI classes themselves (top), and for the GmI classes (bottom). Scenarios are described in Section 4.4 and discussed in Section 5.3.

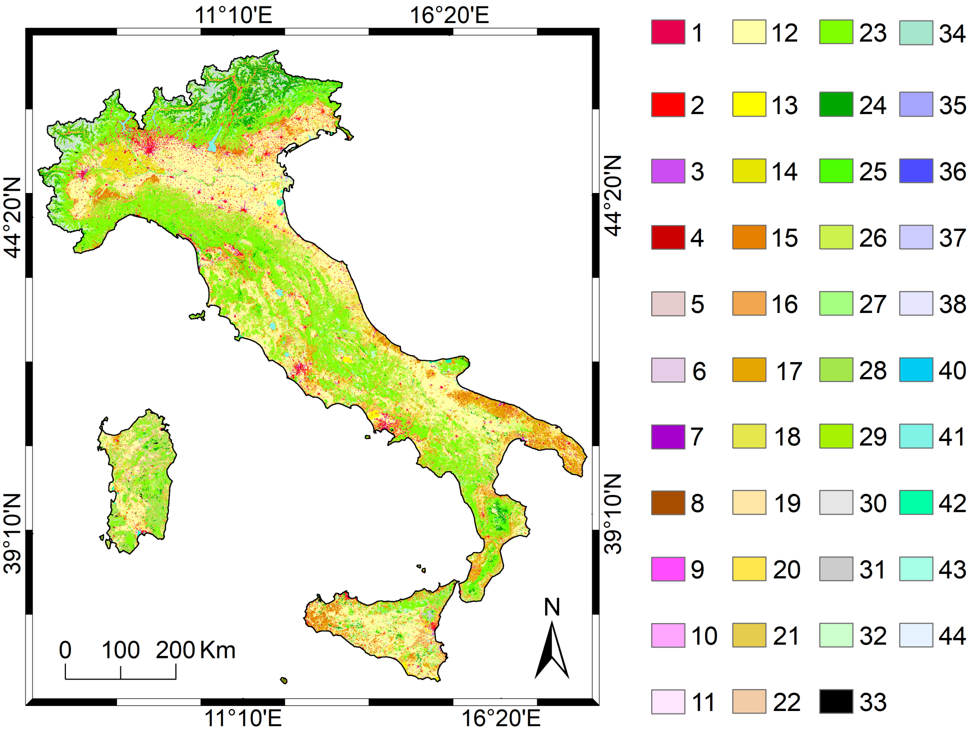

Figure 1: CORINE Land Cover class distribution on the whole of Italy; data correspond to the 2018 release, and classes match those listed in Table 2, last column, and are defined as follows: 1: Continuous urban fabric. 2: Discontinuous urban fabric. 3: Industrial or commercial units. 4: Road and rail networks and associated land. 5: Port areas. 6: Airports. 7: Mineral extraction sites. 8: Dump sites. 9: Construction sites. 10: Green urban areas. 11: Sport and leisure facilities. 12: Non-irrigated arable land. 13: Permanent irrigated land. 14: Rice fields. 15: Vineyards. 16: Fruit trees and berry plantations. 17: Olive groves. 18: Pastures. 19: Annual crops associated with permanent crops. 20: Complex cultivation patterns. 21: Land principally occupied by agriculture, with significant areas of natural vegetation. 22: Agro–forestry areas. 23: Broad–leaved forest. 24: Coniferous forest. 25: Mixed forest. 26: Natural grassland. 27: Moors and heathland. 28: Sclerophyllous vegetation. 29: Transitional woodland–shrub. 30: Beaches, dunes, sands. 31: Bare rocks. 32: Sparsely vegetated areas. 33: Burnt areas. 34: Glaciers and perpetual snow. 35: Inland marshes. 36: Peat bogs. 37: Salt marshes. 38: Salines. 39: Intertidal flats. 40: Water courses. 41: Water bodies. 42: Coastal lagoons. 43: Estuaries. 44: Sea and ocean.

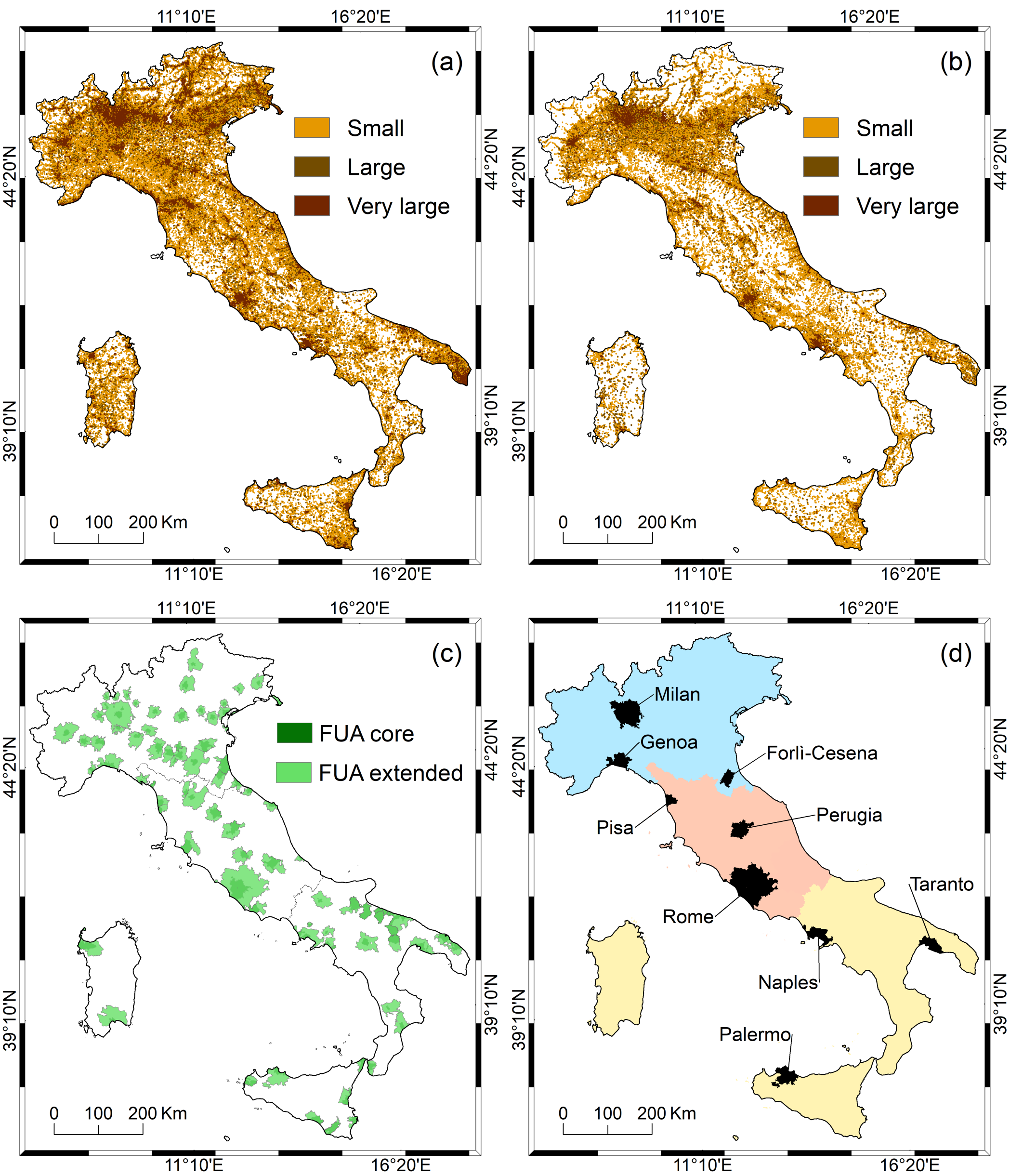

Figure 2: The three definitions of urban boundaries based on different parameters, described in Section 8. (a) UA1, obtained with a parameter–free approach by Alvioli (2020a); (b) UA2, obtained by Alvioli (2020b) from an imperviousness layer by Copernicus; (c), $\mathrm{UA3}_{\mathrm{core}}$ and $\mathrm{UA3}_{\mathrm{ext}}$, corresponding to *core* and *extended* functional urban areas; (d) the official North–Center–South distinction of Italy, and $\mathrm{UA3}_{\mathrm{ext}}$ considered for quantitative assessment in this work.

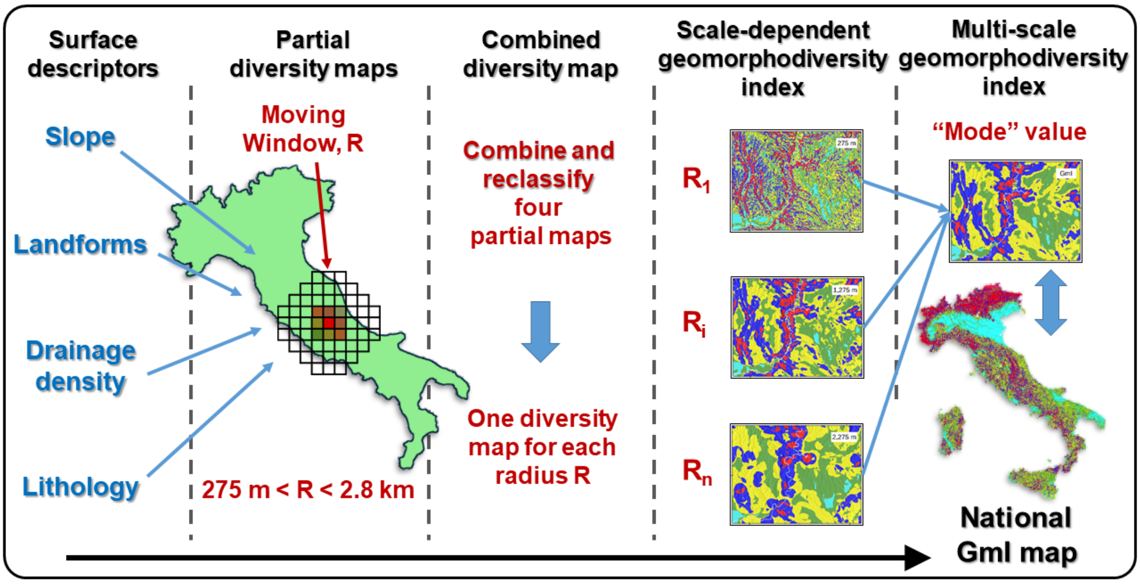

Figure 3: The workflow leading to the high–resolution geomorphodiversity map (GmI) of Italy. The different steps, form left to right, depict: (1) input data, (2) parametric calculation of partial diversity using moving windows, (3) combination of partial maps into as many GmI maps as the values of the parameter R (moving window radius), representing (4) an ensemble, scale–dependent geomorphodiversity assessment, and (5) scale–independent assessment of GmI selecting cell–by–cell most common value of the index across the ensemble. Refer to Section 4.1 for additional details.

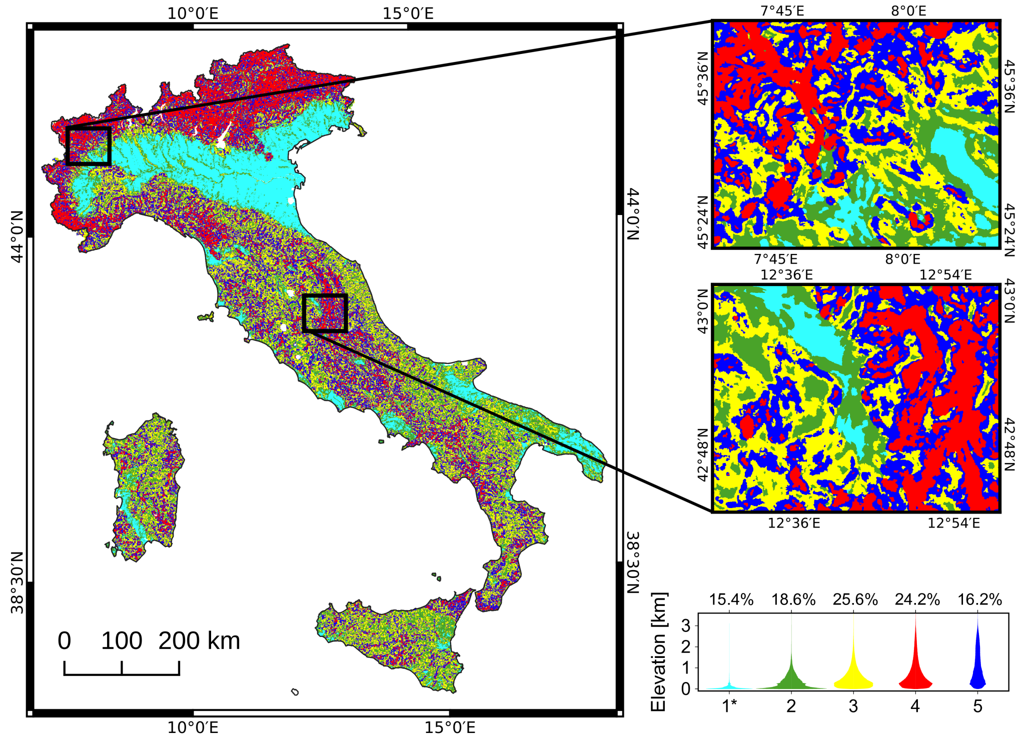

Figure 4: The main map shows the land surface diversity index (GmI) at 25 m resolution, describing the level of geomorphodiversity from 1 (lowest class) to 5 (highest class). Insets are sample areas representative of regions with all GmI classes. Violin plots show the distribution of elevation in each class; colors match the maps. The horizontal range of class GmI = 1 was scaled down by a factor five, w.r.t. other classes; percentages on top horizontal axis are the areal coverage.

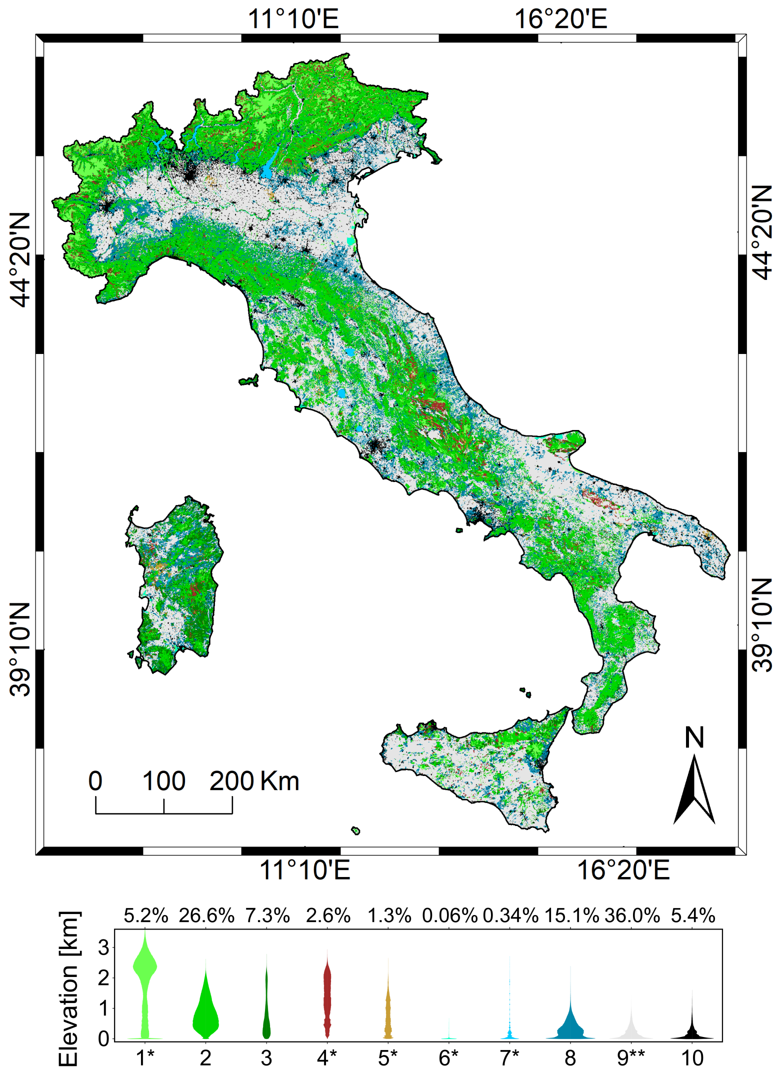

Figure 5: Geographical distribution of the anthropization index, AzI, defined in this work, as described in Section 8. Violin plots show the distribution of elevation in each class; colors match the map classes. One asterisk: horizontal range scaled up by a factor five; two asterisks: scaled down by a factor five. Percentages on top horizontal axis are the areal coverage.

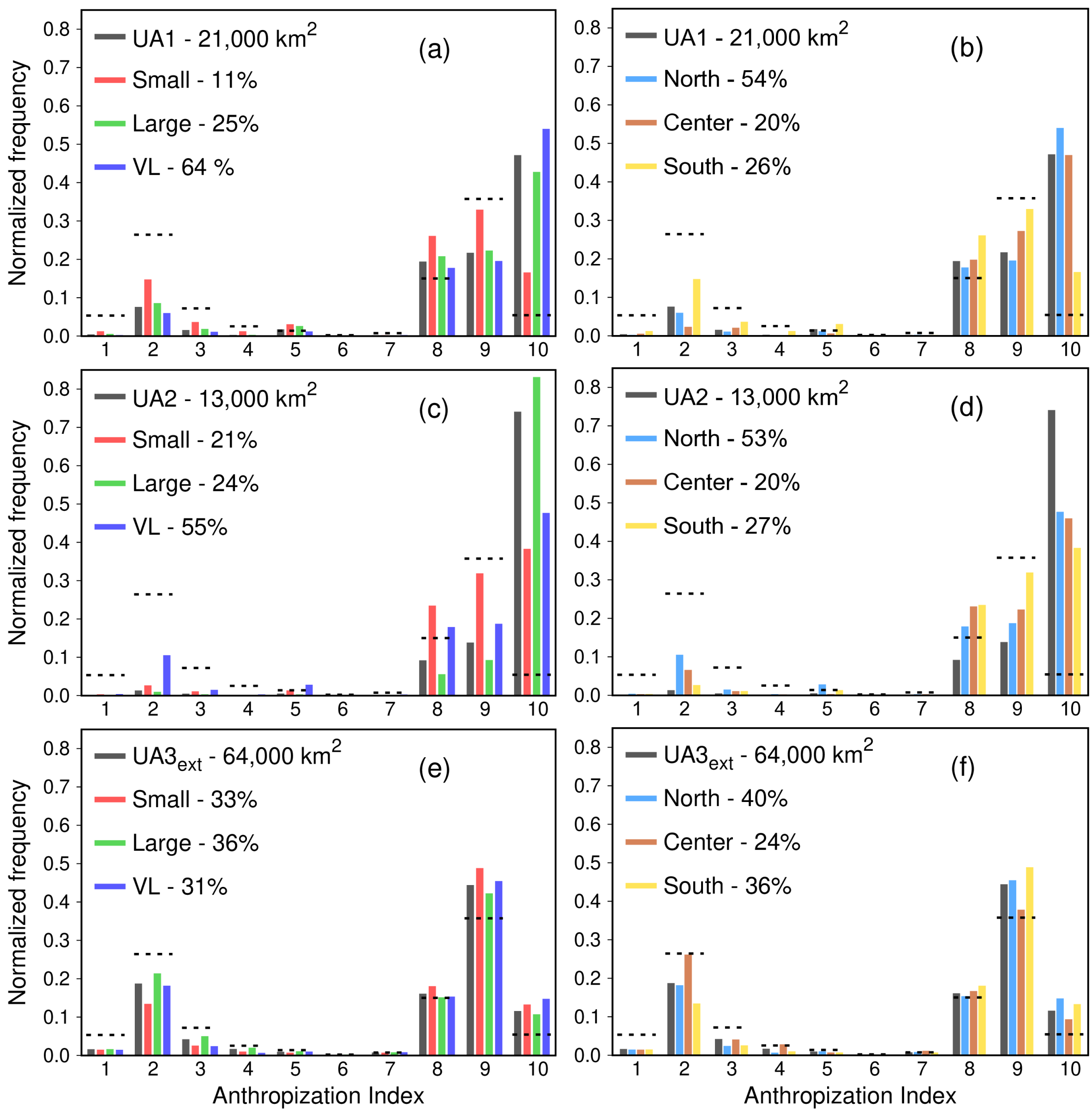

Figure 6: Distribution of AzI classes within the three urban boundaries considered in this work (*cf.* Section 3). Panels (a), (c) and (e) distinguish UAs by their size, and (b), (d) and (f) by their geographical location. The horizontal dotted lines represent the national value, in each class.

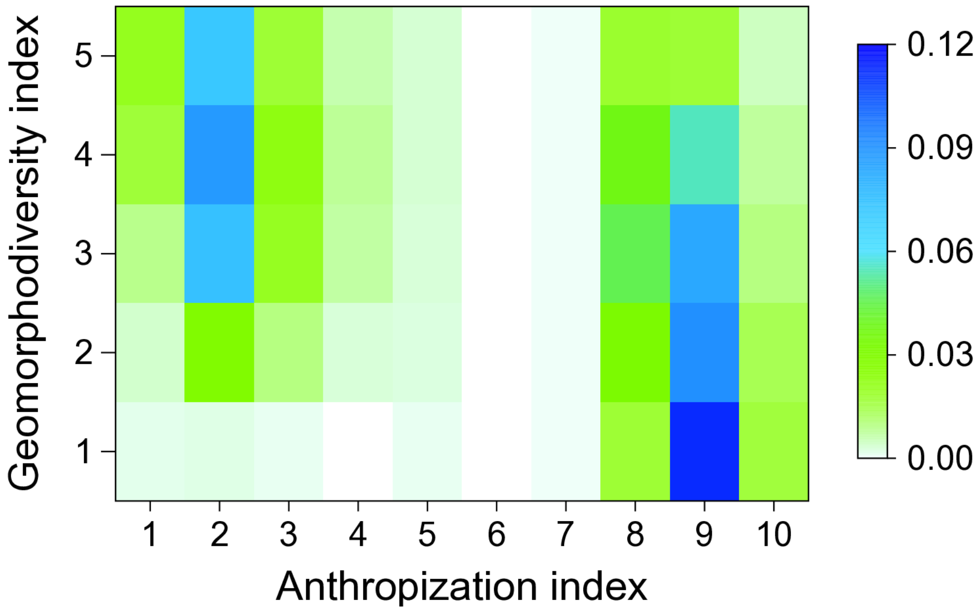

Figure 7: A bivariate diagram showing the degree of anthropization and geomorphodiversity in Italy, represented by the fraction of surface area under each combination of GmI–AzI classes.

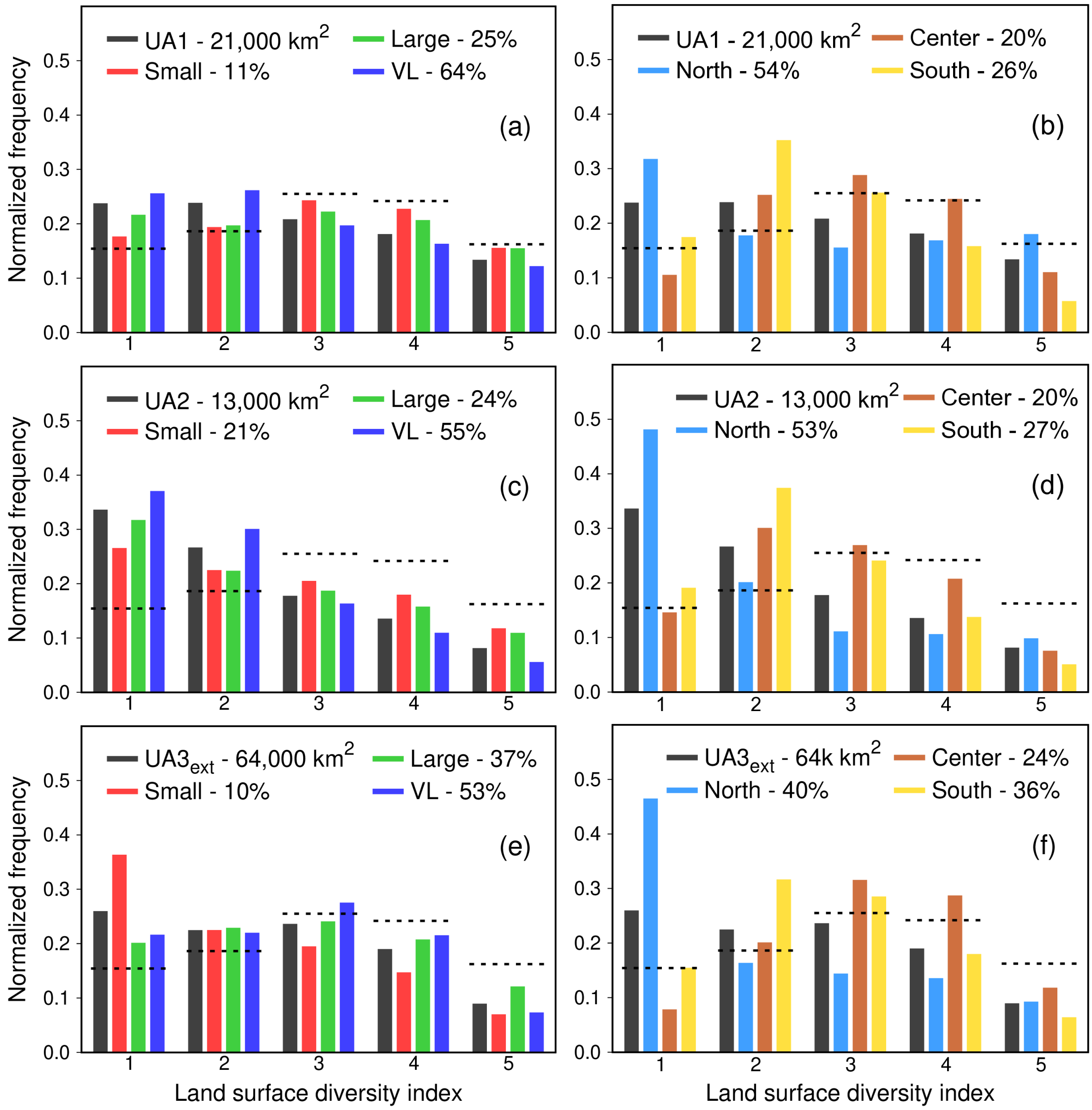

Figure 8: Distribution of GmI classes within the three urban boundaries considered in this work (*cf.* Section 3). Panels (a), (c) and (e) distinguish UAs by their size, and (b), (d) and (f) by their geographical location. The horizontal dotted lines represent the national value, in each class.

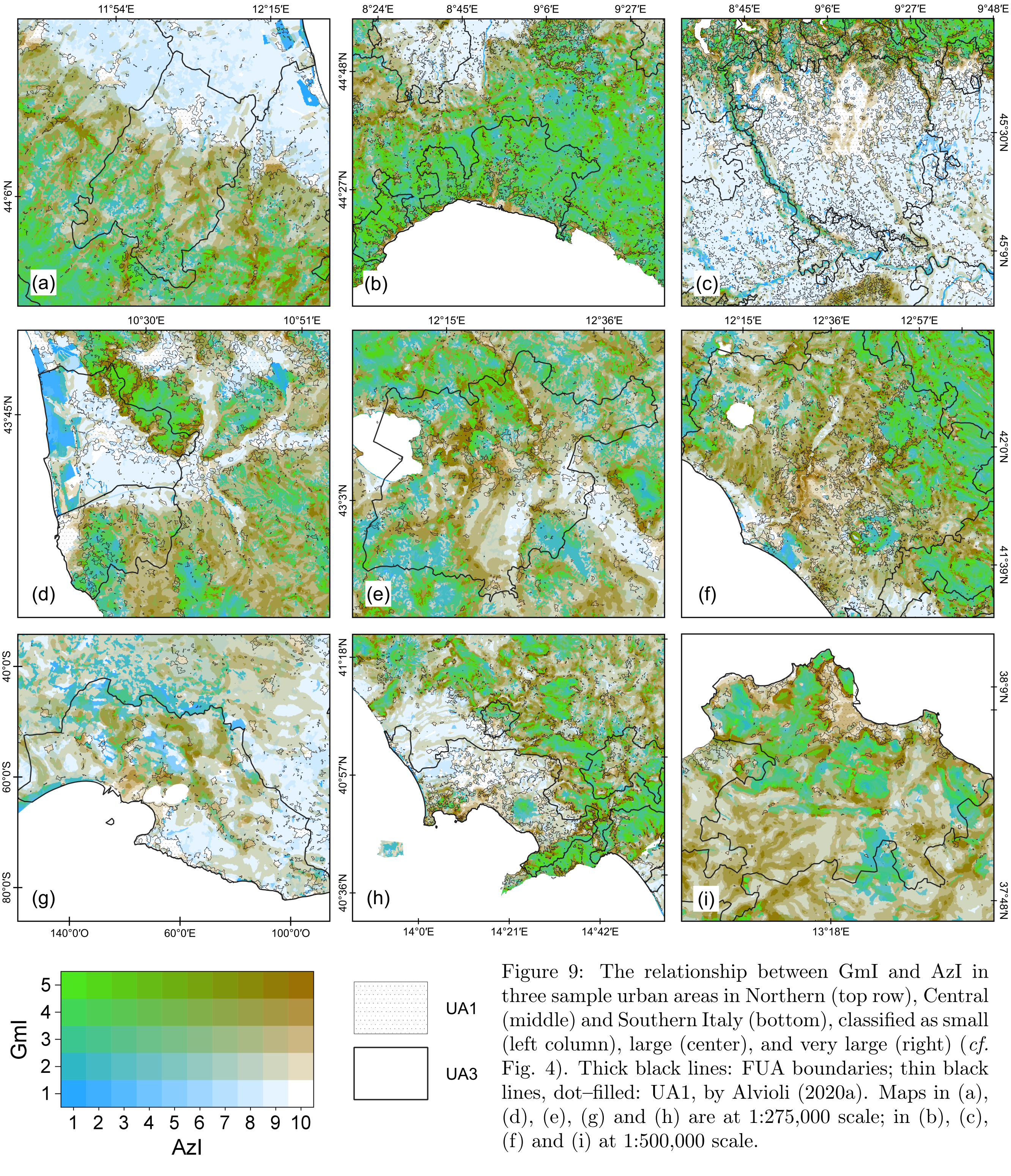

Figure 9: The relationship between GmI and AzI in three sample urban areas in Northern (top row), Central (middle) and Southern Italy (bottom), classified as small (left column), large (center), and very large (right) (*cf.* Fig. 4). Thick black lines: FUA boundaries; thin black lines, dot–filled: UA1, by Alvioli (2020a). Maps in (a), (d), (e), (g) and (h) are at 1:275,000 scale; in (b), (c), (f) and (i) at 1:500,000 scale.

References

Agrawal, N., Dixit, J., 2024. An assessment of the geomorphodiversity and land use/cover change (LUCC) effects associated with landslides in Meghalaya, India. Earth Surface Processes and Landforms , 1468–1482doi:10.1002/esp.5769.

Alvioli, M., 2020a. Administrative boundaries and urban areas in Italy: A perspective from scaling laws. Landscape and Urban Planning 204, 103906. doi:10.1016/j.landurbplan.2020.103906.

Alvioli, M., 2020b. Comparative study of delineation of urban areas using imperviousness products and open data, in: Alvioli, M., Marchesini, I., Melelli, L., Guth, P. (Eds.), Proceedings of the Geomorphometry 2020 Conference, CNR Edizioni, P.le Aldo Moro 7, Roma. pp. 1–4. doi:10.30437/geomorphometry2020_1.

Benito-Calvo, A., Pérez-González, A., Magri, O., Meza, P., 2009. Assessing regional geodiversity: the Iberian Peninsula. Earth Surface Processes and Landforms 34, 1433–1445. doi:10.1002/esp.1840.

Bettencourt, L.M.A., 2013. The origins of scaling in cities. Science 340, 1438–1441. doi:10.1126/science.1235823.

Bettencourt, L.M.A., Lobo, J., Helbing, D., Kühnert, C., West, G.B., 2007. Growth, innovation, scaling, and the pace of life in cities. Proceedings of the National Academy of Sciences 104, 7301–7306. doi:10.1073/pnas.0610172104.

Brandolini, P., Cappadonia, C., Luberti, G., Donadio, C., Stamatopoulos, L., Di Maggio, C., Faccini, F., Stanislao, C., Vergari, F., Paliaga, G., Agnesi, V., Alevizos, G., Del Monte, M., 2020. Geomorphology of the Anthropocene in Mediterranean urban areas. Progress in Physical Geography: Earth and Environment 44, 461–494. doi:10.1177/0309133319881108.

Bucci, F., Santangelo, M., Fongo, L., Alvioli, M., Cardinali, M., Melelli, L., Marchesini, I., 2022. A new digital lithological map of Italy at the 1 : 100 000 scale for geomechanical modelling. Earth System Science Data 14, 4129–4151. doi:10.5194/essd-14-4129-2022.

Burnelli, M., Melelli, L., Alvioli, M., 2023. Land surface diversity: A geomorphodiversity index of Italy. Earth Surface Processes and Landforms 48, 3025–3040. doi:10.1002/esp.5679.

Burnelli, M., Pica, A., Del Monte, M., Delchiaro, M., Melelli, L., Reame, F., Alvioli, F.V.M., 2024. Does anthropogenic morphogenesis alter geomorphodiversity in urban environments? Under review .

Chakraborty, A., Gray, M., 2020. A call for mainstreaming geodiversity in nature conservation research and praxis. Journal for Nature Conservation 56, 125862. doi:10.1016/j.jnc.2020.125862.

Coratza, P., Hobléa, F., 2018. Chapter 5 – the specificities of geomorphological heritage, in: Reynard, E., Brilha, J. (Eds.), Geoheritage. Elsevier, pp. 87–106. doi:10.1016/B978-0-12-809531-7.00005-8.

Cottineau, C., Hatna, E., Arcaute, E., Batty, M., 2017. Diverse cities or the systematic paradox of urban scaling laws. Computers, Environment and Urban Systems 63, 80–94. doi:10.1016/j.compenvurbsys.2016.04.006.

Elmqvist, T., Andersson, E., McPhearson, T., Bai, X., Bettencourt, L., Brondizio, E., J. Colding, G.D., Folke, C., Grimm, N., Haase, D., Ospina, D., Parnell, S., Polasky, S., Seto, K.C., Leeuw, S.V.D., 2021. Urbanization in and for the Anthropocene. njp Urban Sustainability 1, 6. doi:10.1038/s42949-021-00018-w.

Evans, I.S., 2012. Geomorphometry and landform mapping: What is a landform? Geomorphology 137, 94–106. doi:10.1016/j.geomorph.2010.09.029. geospatial Technologies and Geomorphological Mapping Proceedings of the 41st Annual Binghamton Geomorphology Symposium.

Feranec, J., Soukup, T., Hazeu, G., Jaffrain, G., 2016. European Landscape Dynamics, CORINE Land Cover data. CRC Press.

Fox, N., Graham, L.J., Eigenbrod, F., Bullock, J.M., Parks, K.E., 2020. Incorporating geodiversity in ecosystem service decisions. Ecosystems and People 16, 151–159. doi:10.1080/26395916.2020.1758214.

Gray, M., 2008. Geodiversity: developing the paradigm. Proceedings of the Geologists' Association 119, 287–298. doi:10.1016/S0016-7878(08)80307-0.

Hamilton, R., Rae, A., 2020. Regions from the ground up: a network partitioning approach to regional delineation. Environment and Planning B: Urban Analytics and City Science 47, 775–789. doi:10.1177/2399808318804226.

Hartmann, J., Moosdorf, N., 2012. The new global lithological map database GLiM: A representation of rock properties at the Earth surface. Geochemistry, Geophysics, Geosystems 13. doi:10.1029/2012GC004370.

Hiwahashi, J., Yamazaki, D., 2022. Global polygons for terrain classification divided into uniform slopes and basins. Progress in Earth and Planetary Science 9, 33. doi:10.1186/s40645-022-00487-2.

Howard, A.D., 1965. Geomorphological systems; equilibrium and dynamics. American Journal of Science 263, 302–312. doi:10.2475/ajs.263.4.302.

Jasiewicz, J., Stepinski, T., 2013. Geomorphons – a pattern recognition approach to classification and mapping of landforms. Geomorphology 182, 147–156. doi:10.1016/j.geomorph.2012.11.005.

Jiang, B., Liu, X., 2012. Scaling of geographic space from the perspective of city and field blocks and using volunteered geographic information. International Journal of Geographical Information Science 26, 215–229. doi:10.1080/13658816.2011.575074.

Kubalíková, L., Coratza, P., 2023. Reflections of geodiversity–culture relationships within the concept of abiotic ecosystem services. Geological Society, London, Special Publications 530, 49–66. doi:10.1144/SP530-2022-155.

Leopold, L.B., Wolman, M.G., Miller, J.P., Wohl, E.E., 2020. Fluvial processes in geomorphology. Courier Dover Publications.

Lima Magalhães, J., Lopes, M., Lima de Queiroz, H., 2015. Development of a Flooded Forest Anthropization Index (FFAI) applied to Amazonian areas under pressure from different human activities. Ecological Indicators 48, 440–447. doi:10.1016/j.ecolind.2014.09.002.

Marchetti, M., Soldati, M., Vandelli, V., 2017. The great diversity of italian landscapes and landforms: Their origin and human imprint, in: Soldati, M., Marchetti, M. (Eds.), Landscapes and Landforms of Italy. Springer, Cham.. World Geomorphological Landscapes, pp. 7–20. doi:10.1007/978-3-319-26194-2_2.

Masucci, A.P., Arcaute, E., Hatna, E., Stanilov, K., Batty, M., 2015. On the problem of boundaries and scaling for urban street networks. Journal of The Royal Society Interface 12, 20150763. doi:10.1098/rsif.2015.0763.

McDonald, R.I., Beatley, T., Elmqvist, 2018. The green soul of the concrete jungle: the urban century, the urban psychological penalty, and the role of nature. Sustainable Earth 1, 3. doi:10.1186/s42055-018-0002-5.

Melelli, L., Vergari, F., Liucci, L., Del Monte, M., 2017. Geomorphodiversity index: Quantifying the diversity of landforms and physical landscape. Science of The Total Environment 584-585, 701–714. doi:10.1016/j.scitotenv.2017.01.101.

United Nations, 2015. Transforming our world: the 2030 agenda for sustainable development. https://www.refworld.org/legal/resolution/unga/2015/en/111816. A/RES/70/1.

United Nations, 2018. The World's Cities in 2018. Department of Economic and Social Affairs, Population Division. Data booklet, ST/ESA/SER.A/417.

Neteler, M., Mitasova, H., 2008. Open Source GIS: a GRASS GIS approach. Springer New York.

Panizza, M., 2009. The geomorphodiversity of the Dolomites (Italy): A key of geoheritage assessment. Geoheritage 1, 33–42. doi:10.1007/s12371-009-0003-z.

Pelfini, M., Bollati, I., Giudici, M., Pedrazzini, T., Sturani, M., Zucali, M., 2018. Urban geoheritage as a resource for earth sciences education: examples from milan metropolitan area. Rendiconti Online della Società Geologica Italiana 45, 83–88. doi:10.3301/ROL.2018.33.

Pica, A., Melelli, L., Burnelli, M., Del Monte, M., Vergari, F., Alvioli, M., 2024. Geomorphodiversity indices and geomorphological mapping: complementary contributions to landscape classification in urban areas, in: EGU General Assembly 2024, Copernicus. pp. EGU24–20385. doi:10.5194/egusphere-egu24-20385.

Rahbek, C., Borregaard, M., Colwell, R., Dalsgaard, B., Holt, B., Morueta-Holme, N., Nogues-Bravo, D., Whittaker, R., Fjelds, J., 2019. Humboldt's enigma: What causes global patterns of mountain biodiversity? Science 365, 1108–1113. doi:10.1126/science.aax0149.

Reynard, E., Pica, A., Coratza, P., 2017. Urban geomorphological heritage. an overview. Quaestiones Geographicae 36, 7–20. doi:10.1515/quageo-2017-0022.

Rosa, F., van Bodegom, P., Hellweg, S., Pfister, S., Biurrun, I., Boch, S., Chytry, M., Ćušterevska, R., Fratte, M.D., Damasceno, G., Garbolino, E., Lenoir, J., Ozinga, W.A., Penuelas, J., Sabatini, F.M., Schrodt, F., Uogintas, D., Byun, C., Dolezal, J., Dziuba, T., Herault, B., Martfn-Fores, I., Niinemets, U., Peyre, G., Scherer, L., 2024. Land-use impacts on plant functional diversity throughout Europe. bioRxiv doi:10.1101/2024.02.21.580945.

Santangelo, M., Marchesini, I., Bucci, F., Cardinali, M., Cavalli, M., Crema, S., Marchi, L., Alvioli, M., Guzzetti, F., 2021. Exposure to landslides in rural areas in Central Italy. Journal of Maps 17, 124–132. doi:10.1080/17445647.2020.1746699.

Sarretta, A., Minghini, M., 2021. Towards the integration of authoritative and OpenStreetMap geospatial datasets in support of the European strategy for data. The International Archives of the Photogrammetry, Remote Sensing and Spatial Information Sciences XLVI-4/W2-2021, 159–166. doi:10.5194/isprs-archives-XLVI-4-W2-2021-159-2021.

Schiavina, M., Melchiorri, M., Freire, S., Florio, P., Ehrlich, D., Tommasi, P., Pesaresi, M., Kemper, T., 2022. Land use efficiency of functional urban areas: Global pattern and evolution of development trajectories. Habitat International 123, 102543. doi:10.1016/j.habitatint.2022.102543.

Schrodt, F., Bailey, J., Kissling, W., Rijsdijk, K., Seijmonsbergenc, A., van Reed, D., Hjortf, J., Lawleyg, R., William, C., Andersonh, M., Beieri, P., van Beukeringe, P., Boyda, D., Brilhaj, J., Carcavilla, L., Dahlin, K., Gill, J., Gordon, J., Gray, M., Grundy, M., Hunter, M., Lawler, J., Monge-Ganuzass, M., Royseg, K., Stewart, I., Record, S., Turner, W., Zarnetske, P., Field, R., 2019. To advance sustainable stewardship, we must document not only biodiversity but geodiversity. Proceedings of the National Academy of Sciences 116, 16155–16158. doi:10.1073/pnas.1911799116.

Shi, K.S., Yu, B., Ma, J., Cao, W., Cui, Y., 2023. Impacts of slope climbing of urban expansion on global sustainable development. The Innovation 4, 100529. doi:10.1016/j.xinn.2023.100529.

Sofia, G., Roder, G., Dalla Fontana, G., Tarolli, P., 2017. Flood dynamics in urbanised landscapes: 100 years of climate and humans' interaction. Scientific Reports 7, 40527. doi:10.1038/srep40527.

Stewart, I.S., Gill, J.C., 2017. Social geology – integrating sustainability concepts into Earth sciences. Proceedings of the Geologists' Association 128, 165–172. doi:10.1016/j.pgeola.2017.01.002.

Tarolli, P., Sofia, G., 2016. Human topographic signatures and derived geomorphic processes across landscapes. Geomorphology 255, 140–161. doi:10.1016/j.geomorph.2015.12.007.

Thornbush, M.J., Allen, C.D., 2018. Urban Geomorphology. Elsevier. doi:10.1016/C2016-0-02169-1.

Tukiainen, H., Toivanen, M., Maliniemi, T., 2023. Geodiversity and biodiversity. Geological Society, London, Special Publications 530, 31–47. doi:10.1144/SP530-2022-107.

Vačkář, D., ten Brink, B., Loh, J., Baillie, J.E., Reyers, B., 2012. Review of multispecies indices for monitoring human impacts on biodiversity. Ecological Indicators 17, 58–67. doi:10.1016/j.ecolind.2011.04.024. indicators of environmental sustainability: From concept to applications.

Vergari, F., Pica, A., andLaura Melelli, P.B., Del Monte, M., 2022. Geomorphological classification of the landscape in urban areas: hints from some study cases in italy. Rendiconti Online della Società Geologica Italiana 57, 33–39. doi:10.3301/ROL.2022.09.

WCS, W.C.S., CIESIN, C.f.I.E.S.I.N., 2005. Last of the Wild Project, v.2 (lwp-2): Global Human Influence Index Dataset. doi:10.7927/H4BP00QC.

Zumpano, V., Ardizzone, F., Bucci, F., Cardinali, M., Fiorucci, F., Parise, M., Pisano, L., Reichenbach, P., Santaloia, F., Santangelo, M., Wasowski, J., Lollino, P., 2021. The relation of spatio–temporal distribution of landslides to urban development (a case study from the Apulia region, Southern Italy). Journal of Maps 17, 133–140. doi:10.1080/17445647.2020.1746417.

Zwoliński, Z., Najwer, A., Giardino, M., 2018. Chapter 2 – Methods for assessing geodiversity, in: Reynard, E., Brilha, J. (Eds.), Geoheritage. Elsevier, pp. 27–52. doi:10.1016/B978-0-12-809531-7.00002-2.